PROCEEDINGS OF SCIENCE

CP violation and branching fraction measurements in *B* decays to open charm final states

Fionn Bishop[*] **on behalf of the LHCb collaboration**

Laboratoire d'Annecy de Physique des Particules,
9 Chemin de Bellevue, Annecy, France

E-mail: fionn.caitlin.ros.bishop@cern.ch

The latest measurements of charge-parity violation and branching fractions in beauty hadron decays to open charm final states using data collected by the LHCb detector in 2011-18 are reviewed. These results help to constrain theories beyond the Standard Model of particle physics, and improve our understanding of QCD dynamics in beauty hadron decays including rescattering effects and factorisation.

The European Physical Society Conference on High Energy Physics (EPS-HEP2023)
21-25 August 2023
Hamburg, Germany

[*]Speaker

PoS(EPS-HEP2023)339

1. Introduction

Measurements of the open charm decays of beauty hadrons are useful to test the Standard Model (SM) and thereby provide sensitivity to physics beyond the SM (BSM), and to improve our understanding of non-perturbative quantum chromodynamics (QCD). Three measurements on this topic are presented using data collected by the LHCb experiment, a forward spectrometer at the Large Hadron Collider with excellent particle identification, tracking, and momentum resolution capabilities [1].

2. *CP* asymmetries and branching fractions of B^- decays to two charm mesons

Charge-parity (*CP*) asymmetries arise in doubly charmed B^- decays due to interference between the contributions from tree, QCD penguin, and annihilation diagrams (Figure 1). The QCD penguin diagram amplitudes are not well known, but correlations in *CP* asymmetries and branching fractions between doubly charmed B^-, B^0, and B^0_s decays can be predicted with small hadronic uncertainties regardless. Testing these correlations could allow enhancements to the *CP* asymmetries from BSM physics to be identified [2]. The *CP* asymmetries

$$\mathcal{A}^{CP} \equiv \frac{\Gamma(B^- \to D^{(*)-}_{(s)} D^{(*)0}) - \Gamma(B^+ \to D^{(*)+}_{(s)} \overline{D}^{(*)0})}{\Gamma(B^- \to D^{(*)-}_{(s)} D^{(*)0}) + \Gamma(B^+ \to D^{(*)+}_{(s)} \overline{D}^{(*)0})} \tag{1}$$

are measured for seven decays using data corresponding to 9 fb^{-1} of proton-proton (pp) collisions [3] by subtracting the charge asymmetries of B^- meson production and final state particle detection from the charge asymmetry of the signal decay yields in the data sample.

Decays involving one D_s^{*-} or D^{*0} mesons are partially reconstructed in their decay to a D_s^- or D^0 meson, respectively, plus a soft neutral particle that is not reconstructed. Other charm mesons are reconstructed through the $D^0 \to K^-\pi^+$, $D^0 \to K^-\pi^+\pi^-\pi^+$, $D^- \to K^+\pi^-\pi^-$, $D_s^- \to K^-K^+\pi^-$ and $D^{*-} \to \overline{D}^0\pi^-$ decays.

Backgrounds from random combinations of tracks and specific decay modes are reduced with selections on the kinematic, geometric, and particle identification properties of the candidates. The raw yields are obtained in an extended maximum likelihood (EML) fit to the invariant mass distribution of data candidates (Figure 2). The charge-summed yields of the fully reconstructed decays are $N(D_s^- D^0) = 230\,500 \pm 500$, $N(D^- D^0) = 11\,490 \pm 120$ and $N(D^{*-} D^0) = 3\,100 \pm 70$.

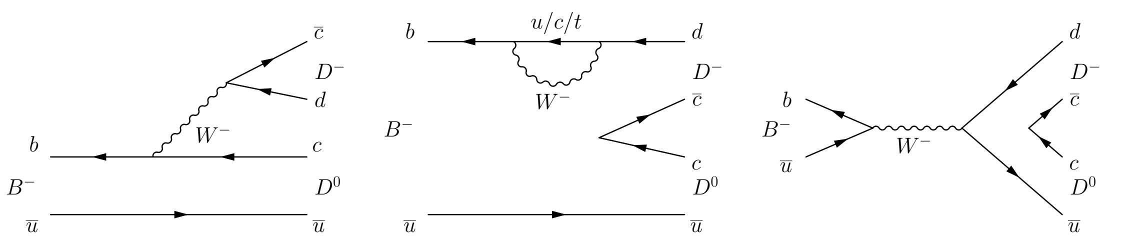

Figure 1: (Left) tree, (centre) QCD penguin, and (right) annihilation diagrams contributing to the $B^- \to D^- D^0$ decay in the SM.

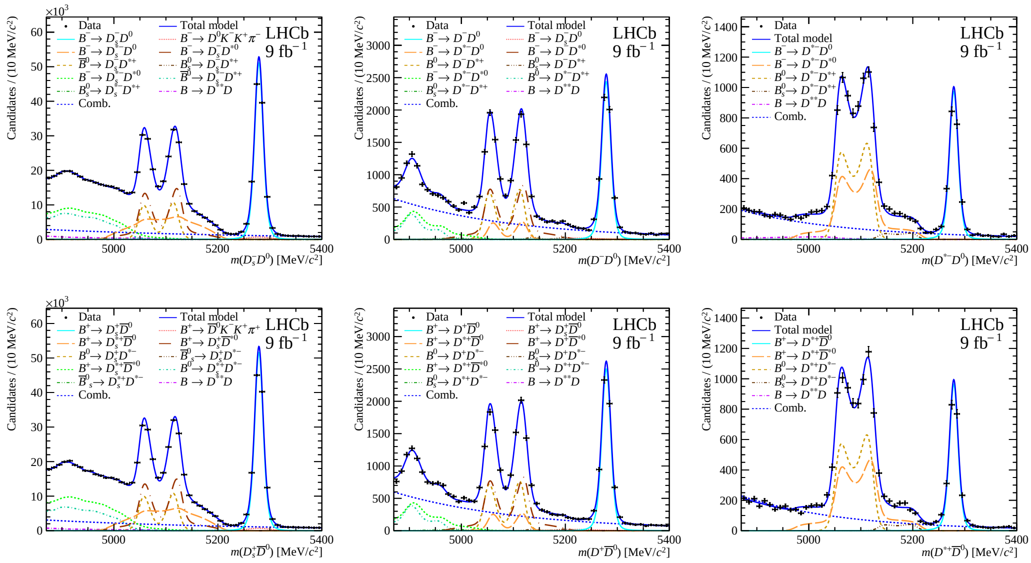

Figure 2: Invariant-mass distribution of (left) $B^- \to D_s^- D^0$ candidates, (centre) $B^- \to D^- D^0$ candidates and (right) $B^- \to D^{*-} D^0$ candidates, separated by charge into (top row) B^- and (bottom row) B^+ candidates. A model fitted to describe the distribution is also drawn.

The production asymmetry has been measured as a function of the transverse momentum and rapidity of the $B^\pm$ meson and the centre-of-mass energy of the pp collisions ($\sqrt{s}$) in the LHCb acceptance using $B^+ \to J/\psi K^+$ decays and was found to equal $(-0.7 \pm 0.3)\%$ at $\sqrt{s} = 13\,\text{TeV}$ when integrating over the kinematic distribution of the decay [4]. Contributions from the hardware trigger; particle identification; and the nuclear interactions, reconstruction, and acceptance of the final state particles are considered in the detection asymmetry. Each source is evaluated using large beauty or charm calibration samples, and are all found to be small except for the asymmetry of charged kaon detection, which is up to 1% per kaon.

Additionally, ratios of branching fractions are measured for fully reconstructed decays from the ratio of the efficiency corrected yields,

$$R(D^- D^0 / D_s^- D^0) \equiv \frac{\mathcal{B}(B^- \to D^- D^0)}{\mathcal{B}(B^- \to D_s^- D^0)} \frac{\mathcal{B}(D^- \to K^+\pi^-\pi^-)}{\mathcal{B}(D_s^- \to K^+K^-\pi^-)} = \frac{N(D^- D^0)}{N(D_s^- D^0)} \frac{\varepsilon(D_s^- D^0)}{\varepsilon(D^- D^0)}, \tag{2}$$

and

$$R(D^{*-} D^0 / D^- D^0) \equiv \frac{\mathcal{B}(B^- \to D^{*-} D^0)}{\mathcal{B}(B^- \to D^- D^0)} \frac{\mathcal{B}(D^{*-} \to \overline{D}^0 \pi^-)\mathcal{B}(\overline{D}^0 \to K^+\pi^-)}{\mathcal{B}(D^- \to K^+\pi^-\pi^-)}, \tag{3}$$

which is evaluated analagously. Efficiencies are evaluated using simulated signal samples with data-driven corrections of up to 6% applied to the hardware trigger, track reconstruction, and particle identification efficiencies.

The measured *CP* asymmetries and branching fraction ratios are

$$\mathcal{A}^{CP}(B^- \to D_s^- D^0) = (+0.5 \pm 0.2 \pm 0.5 \pm 0.3)\%,$$
$$\mathcal{A}^{CP}(B^- \to D_s^{*-} D^0) = (-0.5 \pm 1.1 \pm 1.0 \pm 0.3)\%,$$
$$\mathcal{A}^{CP}(B^- \to D_s^- D^{*0}) = (+1.1 \pm 0.8 \pm 0.6 \pm 0.3)\%,$$

$$\begin{aligned}
\mathcal{A}^{CP}(B^- \to D^- D^0) &= (+2.5 \pm 1.0 \pm 0.4 \pm 0.3)\%, \\
\mathcal{A}^{CP}(B^- \to D^- D^{*0}) &= (-0.2 \pm 2.0 \pm 1.4 \pm 0.3)\%, \\
\mathcal{A}^{CP}(B^- \to D^{*-} D^0) &= (+3.3 \pm 1.6 \pm 0.6 \pm 0.3)\%, \\
\mathcal{A}^{CP}(B^- \to D^{*-} D^{*0}) &= (+2.3 \pm 2.1 \pm 1.7 \pm 0.3)\%, \\
R(D^- D^0/D_s^- D^0) &= (7.25 \pm 0.09 \pm 0.09) \times 10^{-2}, \\
R(D^{*-} D^0/D^- D^0) &= (0.271 \pm 0.007 \pm 0.005),
\end{aligned}$$

where the first uncertainty is statistical, the second is systematic, and the third is from $\mathcal{A}^{CP}(B^+ \to J/\psi K^+)$. These are the most precise $\mathcal{A}^{CP}$ measurements for these decays and the first measurements of $\mathcal{A}^{CP}(B^- \to D_s^{*-} D^0)$ and $\mathcal{A}^{CP}(B^- \to D_s^- D^{*0})$, and will help to constrain BSM physics models.

3. Branching fractions of $B^0_{(s)} \to \overline{D}^{(*)0}\phi$ decays

In the absence of rescattering, the ratio between the branching fractions of the OZI-suppressed W-exchange $B^0 \to \overline{D}^{(*)0}\phi$ and the tree level $B^0 \to \overline{D}^{(*)0}\omega$ decays (Figure 3, left and centre) is proportional to $\tan^2\delta$, where δ is the $\phi - \omega$ mixing angle. This allows the size of rescattering in $B^0 \to \overline{D}^{(*)0}\phi$ decays to be probed [5]. This search for the $B^0 \to \overline{D}^{(*)0}\phi$ decays [6] uses data corresponding to 9 fb^{-1} of pp collisions. The $\overline{D}^0$ meson is reconstructed in its decay to $K^+\pi^-$ and the $\overline{D}^{*0}$ is partially reconstructed as a $\overline{D}^0$. Branching and polarisation fractions (f_L) of $B_s^0 \to \overline{D}^{(*)0}\phi$ decays (Figure 3, right) are also measured; future measurements of the untagged *CP* violation of these decays could be used to determine the Cabbibo-Kobayashi-Maskawa (CKM) phase γ [7].

Branching fractions are measured relative to $\mathcal{B}(B^0 \to \overline{D}^0 K^+ K^-)$ from the efficiency-corrected yield ratios. Weights to extract data candidates containing a ϕ resonance are determined with the sPlot technique [9] from a fit to the $m(K^+K^-)$ distribution. Signal and normalisation yields are extracted from EML fits to the weighted and unweighted $m(\overline{D}^0 K^+ K^-)$ distributions, respectively (Figure 4). Efficiencies are evaluated using simulated samples to which data-driven corrections of the efficiencies and Dalitz plot distribution are applied.

Yields of 126 ± 33 and 272 ± 57 are observed for the $B^0 \to \overline{D}^0\phi$ and $B^0 \to \overline{D}^{*0}\phi$ decays corresponding to significances of 3.6 and 4.2 standard deviations, respectively, which constitutes the first evidence for both decays. Values of $\mathcal{B}(B^0 \to \overline{D}^0\phi) = (7.7 \pm 2.1 \pm 0.7 \pm 0.7) \times 10^{-7}$ and $\mathcal{B}(B^0 \to \overline{D}^{*0}\phi) = (2.2 \pm 0.5 \pm 0.2 \pm 0.2) \times 10^{-7}$ are measured, where the first uncertainty is statistical, the second systematic, and the third from input branching fractions. These values correspond to $\tan^2\delta = (3.6 \pm 0.7 \pm 0.4) \times 10^{-3}$, which is consistent with the absence of large contributions from rescattering [5]. Values of $\mathcal{B}(B_s^0 \to \overline{D}^0\phi) = (2.30 \pm 0.10 \pm 0.11 \pm 0.20) \times 10^{-5}$,

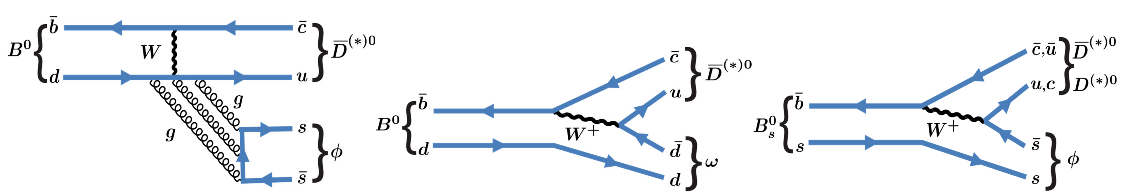

Figure 3: Dominant diagrams for the (left) $B^0 \to \overline{D}^{(*)0}\phi$, (centre) $B^0 \to \overline{D}^{(*)0}\omega$, and (right) $B_s^0 \to \overline{D}^{(*)0}\phi$ decays [8].

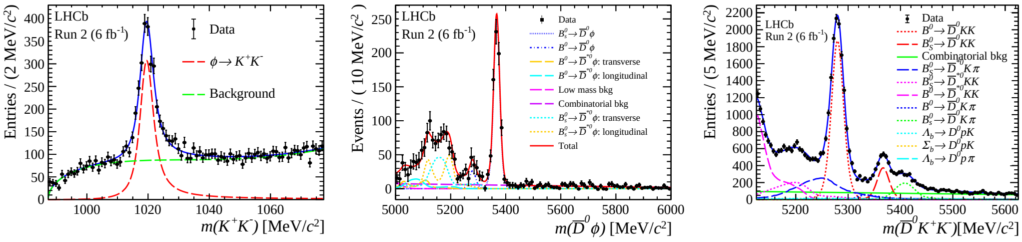

Figure 4: Distributions of (left) $m(K^+K^-)$, (centre) weighted $m(\overline{D}^0\phi)$, and (right) unweighted $m(\overline{D}^0K^+K^-)$ candidates in Run 2 data, and fitted model.

$\mathcal{B}(B_s^0 \to \overline{D}^{*0}\phi) = (3.17 \pm 0.16 \pm 0.17 \pm 0.27) \times 10^{-5}$, and $f_L(B_s^0 \to \overline{D}^{*0}\phi) = (53.1 \pm 6.0 \pm 1.9)\%$ are also measured.

4. Branching fraction of the $\Lambda_b^0 \to D_s^- p$ decay

A measurement of the branching fraction of the tree level $\Lambda_b^0 \to D_s^- p$ decay (Figure 5),

$$\mathcal{B}(\Lambda_b^0 \to D_s^- p) \propto |V_{ub}|^2 |V_{cs}|^2 f_{D_s^+}^2 |F_{\Lambda_b^0 \to p}(m_{D_s^+}^2)|^2 |a_{NF}|^2, \tag{4}$$

combined with better knowledge of the form factor $F_{\Lambda_b^0 \to p}$, allows the extraction of the product $|V_{ub}||a_{NF}|$. The parameter a_{NF} is the relative size of the non-factorisable effects, and its measurement would improve understanding of factorisation in Λ_b^0 baryon decays.

The branching fraction is measured relative to $\mathcal{B}(\Lambda_b^0 \to \Lambda_c^+\pi^-)$ using data corresponding to 6 fb^{-1} of pp collisions from the efficiency-corrected ratio of the yields. Efficiencies are evaluated using simulated samples with data-driven corrections applied. Yields of the signal and normalisation decays are obtained from EML fits to the $m(D_s^- p)$ and $m(\Lambda_c^+\pi^-)$ distributions, respectively (Figure 6). Backgrounds from misidentified decays are reduced using requirements on particle identification variables, and the yields of certain misidentified backgrounds are constrained using fits to $B_s^0 \to D_s^-\pi^+$ and $B_s^0 \to D_s^{\mp}K^{\pm}$ candidates. A measured yield of 831 ± 32 decays constitutes the first observation of the $\Lambda_b^0 \to D_s^- p$ decay. The measured branching fraction is $\mathcal{B}(\Lambda_b^0 \to D_s^- p) = (12.6 \pm 0.5 \pm 0.3 \pm 1.2) \times 10^{-6}$ where the first uncertainty is statistical, the second systematic, and the third from input branching fractions [10].

5. Conclusion

The most recent measurements of open charm decays of beauty hadrons with the LHCb detector have been reviewed. These measurements constrain BSM physics models and improve

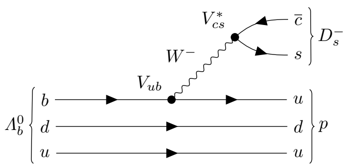

Figure 5: Dominant diagram for the $\Lambda_b^0 \to D_s^- p$ decay.

PoS(EPS-HEP2023)339

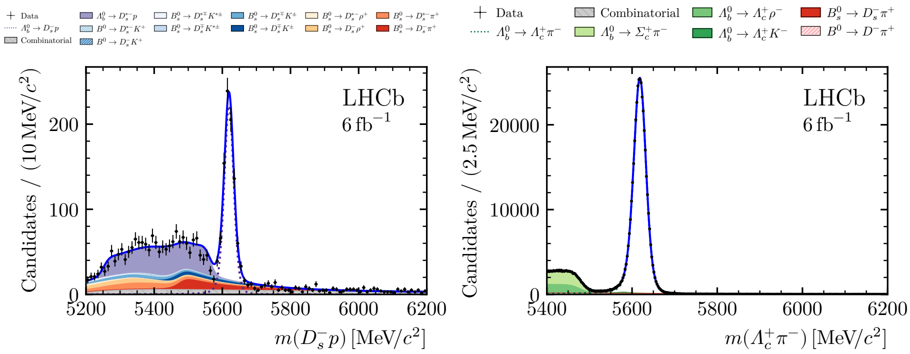

Figure 6: Invariant mass distribution of (left) $D_s^- p$ and (right) $\Lambda_c^+\pi^-$ candidates, and the fitted model.

our understanding of non-perturbative QCD in beauty hadron decays. Many further measurements remain possible with the data collected by the LHCb detector between 2011 and 2018, including measurements of *CP* violation in doubly charmed B^0 meson decays and the CKM phase γ in $B_s^0 \to \overline{D}^{(*)0}\phi$ decays.

References

[1] LHCb collaboration, *The LHCb detector at the LHC*, *JINST* **3** (2008) S08005.

[2] M. Jung and S. Schacht, *Standard model predictions and new physics sensitivity in $B \to DD$ decays*, *Phys. Rev. D* **91** (2015) 034027 [1410.8396].

[3] LHCb collaboration, *Measurement of CP asymmetries and branching fractions of B^- decays to two charm mesons*, *JHEP* **09** (2023) 202 [2306.09945].

[4] LHCb collaboration, *Direct CP violation in charmless three-body decays of $B^\pm$ mesons*, *Phys. Rev.* **D108** (2023) 012008 [2206.07622].

[5] M. Gronau and J.L. Rosner, *B decays dominated by $\omega - \phi$ mixing*, *Phys. Lett. B* **666** (2008) 185 [0806.3584].

[6] LHCb collaboration, *Evidence for the decay $B^0 \to \bar{D}^{(*)0}\phi$ and improved measurements of the branching fractions of the $B_s^0 \to \bar{D}^{(*)0}\phi$ modes*, 2306.02768.

[7] D. Ao et al., *Study of CKM angle γ sensitivity using flavor untagged $B_s^0 \to \tilde{D}^{(*)0}\phi$ decays*, *Chin. Phys. C* **45** (2021) 023003 [2008.00668].

[8] LHCb collaboration, *Observation of the decay $B_s^0 \to \overline{D}^{*0}\phi$ and search for the mode $B^0 \to \overline{D}^0\phi$*, *Phys. Rev.* **D98** (2018) 071103(R) [1807.01892].

[9] M. Pivk and F.R. Le Diberder, *SPlot: A Statistical tool to unfold data distributions*, *Nucl. Instrum. Meth. A* **555** (2005) 356 [physics/0402083].

[10] LHCb collaboration, *First observation and branching fraction measurement of the $\Lambda_b^0 \to D_s^- p$ decay*, *JHEP* **07** (2023) 075 [2212.12574].